

UDC 541.6:547.53

**CONFORMATIONAL ANALYSIS OF 2-ANTHRYLETHYLENE DERIVATIVES:
PHOTOCHEMICAL AND COMPUTATIONAL INVESTIGATION****U. Srinivas¹, P. Arun Kumar¹, Kolupula Srinivas^{2,3}, K. Bhanuprakash², V. Jayathirtha Rao¹**¹*Organic Division-II, Indian Institute of Chemical Technology, Hyderabad, India*²*Inorganic and Physical Chemistry Division, Indian Institute of Chemical Technology, Hyderabad, India,
e-mail: skolupula@niperhyd.ac.in, ksrinivas07@yahoo.com*³*National Institute of Pharmaceutical Education and Research (NIPER), Balanagar, Hyderabad, India**Received November, 5, 2011*

2-Anthrylethylene derivatives **1E**–**5E** and **1Z** are synthesized to study the *cis*–*trans* photoisomerization. Interestingly, unlike 9-anthrylethylene derivatives, 2-anthrylethylene derivatives **1E** to **5E** do not exhibit *E* (*trans*) to *Z* (*cis*) photoisomerization upon direct and triplet sensitization. One-way *Z* (*cis*) to *E* (*trans*) photoisomerization of **1Z** is found to be very efficient under direct and triplet sensitization conditions, demonstrating the involvement of both singlet and triplet states. **1E**–**5E** exhibits excitation wavelength dependent fluorescence indicating the existence of conformers (rotamers) at room temperature, which is confirmed by fluorescence lifetimes measurements of compounds **1E** and **2E**. Theoretical studies are carried out at DFT and *ab initio* methodology and the calculated relative energy difference of the conformers is very small; it ranges between 2.9 kJ·mol⁻¹ to 6.3 kJ·mol⁻¹ for both ground and excited states.

Keywords: 2-anthrylethylene derivatives, photochemical *cis*–*trans* isomerization, fluorescence, charge transfer, conformational analysis, theoretical studies.

INTRODUCTION

The photochemical $Z \rightleftharpoons E$ (*cis* \rightleftharpoons *trans*) isomerization of olefins has been extensively investigated. Much work has been carried out for stilbene and its derivatives [1–18], because of its importance in academia [19, 20], industry [21–24], and biological processes [25–27]. The light-driven *E* (*trans*) to *Z* (*cis*) isomerization of stilbene and other diarylethylenes has been a subject of active investigation because of fundamental [3, 20] and practical applications [8, 28]. Stilbene undergoes conventional efficient two-way isomerization with a weak fluorescence. Strong fluorescence was observed in *trans*-diarylethylenes containing large polyaromatic group such as anthracene, which display only one-way *cis*-to-*trans* isomerization [29–32]. Saltiel *et al.* studied the rotamer dependent *E* (*trans*) to *Z* (*cis*) isomerization in 2-anthrylethylene derivatives [33–36]. Conformational analysis of the vinyl naphthalenes, naphthylacrylic acid and amide derivatives were carried out by Lewis *et al.* [37] by means of NOE and Infrared spectroscopy. The rotational isomerization of 2-anthrylethene in the ground and excited states is a subject of interest in photochemistry [38–44]. Rotamers of (*E*)-2-anthrylethylenes, particularly one-way $Z(cis) \rightarrow E(trans)$ isomerization has been studied using steady-state fluorescence [38, 39], time-correlated single-photon counting (SPC) [39–42], time-gated fluorescence spectroscopy [45, 46], principal component analysis with self-modeling (PCA-SM) [40, 41] and T–T absorption spectroscopy [47, 48]. Despite the literature is abundant with articles related to conformational analysis and or rotamerism [49–58], less attention has been paid towards understanding the photochemical $E(trans) \rightarrow Z(cis)$ isomerization of 2-anthrylethylenes carrying electron withdrawing end groups. Our continuing efforts in studying the photochemical $Z \rightleftharpoons E$ isomerization of various ole-

fins [59—62], led us to investigate the photochemical $Z \rightleftharpoons E$ isomerization of 2-anthrylethylenes derivatives. So we report herein the synthesis, photoisomerization, fluorescence, conformational analysis and computational studies on 2-anthrylethylenes carrying electron withdrawing end groups. 2-Anthrylethylene derivatives **1E** to **5E** did not exhibit $E(\text{trans}) \rightleftharpoons Z(\text{cis})$ photoisomerization upon direct and triplet sensitization conditions, in contrast to the 9-anthrylethylene derivatives [60—62]. However, we found that isomerization can take place exclusively $Z \rightarrow E$ one-way, and without producing any photocyclized product. Steady state fluorescence and fluorescence lifetime experiments indicated the existence of two rotamers. Furthermore, theoretical studies were conducted to estimate the stability of the rotamers in the ground and excited states.

EXPERIMENTAL

A Perkin-Elmer Lambda-2 UV-Visible spectrometer was used to obtain the absorption spectra. A SPEX Fluorolog 0.22 m fluorimeter was used for fluorescence measurements. Mass spectra were recorded on a VG Micro Mass 7070H instrument. Proton nuclear magnetic resonance (^1H NMR) spectra were recorded on a FT-200 MHz and FT-300 MHz instrument in CDCl_3 solvent. A Shimadzu LC-8 HPLC system with a CR-8 integrator was used for HPLC analysis. An Applied Photo Physics QYR-20 Quantum Yield Reactor coupled with a 200 W Hg lamp was used to determine the quantum yields. All other chemicals were purchased from Aldrich/Fluka and locally.

7 (-2-anthracenecarbaldehyde): to a cooled solution of 2-cyanoanthracene **6** (2.03 g, 0.01 mol) in 30 ml of dichloromethane was added DIBALH (14 ml, 0.02 mol) at -78°C . The mixture was stirred for 30 min and at ambient temperature for 5 h. Unreacted DIBALH was quenched with a pinch of $\text{NaF}/\text{H}_2\text{O}$ at 0°C . The supernatant liquid was filtered, extracted with chloroform (3×15 ml). The combined extracts were dried and evaporated under reduced pressure and purified by column chromatography on silica using $\text{AcOEt}/\text{Hexane}$ (3:97) as eluent to give anthracene-2-carbaldehyde **7** as yellow solid. Yield: 90%. $R_f = 0.75$ ($\text{AcOEt}/\text{Hexane}$ 5:95); m.p.: $204\text{—}206^\circ\text{C}$; ^1H NMR (200 MHz; CDCl_3): δ 10.21 (s, 1H, CHO), 8.71—8.42 (m, 3H, Ar), 8.20—7.91 (m, 4H, Ar), 7.58—7.41 (m, 2H, Ar); EI-MS (m/z) (%): 206 (M^+) (35), 176 (14), 149 (100), 76 (8).

1E (methyl(E)-3-(2-anthryl)-2-propenoate): methyl diethylphosphonoacetate (2 g, 11 mmol) in dry DMF (15 ml) was slowly added to a suspension of NaH (264 mg, 11 mmol) in dry DMF (20 ml) at room temperature and it was slowly treated with 2-anthracene carbaldehyde **7** (2.06 g, 10 mmol) in 10 ml DMF. After 4 h of stirring the reaction mixture was quenched with water and extracted with ether, (4×20 ml). The combined extracts were dried, evaporated and the residue was purified by silica gel column chromatography to give pure **1E** as yellow solid. Yield: 80%. $R_f = 0.77$ ($\text{AcOEt}/\text{Hexane}$: 5/95); m.p.: $194\text{—}196^\circ\text{C}$; IR (KBr): $\nu^- = 1713, 1620, 1435, 1245, 1050, 986\text{ cm}^{-1}$; ^1H NMR (200 MHz; CDCl_3): δ 8.40—8.35 (d, 2H, $J = 10.4$ Hz, Ar); 8.04—7.93 (m, 4H, Ar), 7.89—7.81 (d, 1H, $J = 16.0$ Hz, CHCHCO_2Me), 7.65—7.6 (d, 1H, $J = 8.0$ Hz, Ar), 7.48—7.44 (m, 2H, Ar), 6.56—6.48 (d, 1H, $J = 16$ Hz, CHCO_2Me), 3.83 (s, 3 H, CO_2CH_3), ^{13}C NMR (75 MHz; CDCl_3): δ 167.5, 144.8, 132.4, 132.1, 131.7, 131.3, 129.0, 128.1, 127.5, 126.2, 126.1, 125.8, 122.2, 117.7, 51.7; EI-MS (m/z) (%): 262 (M^+) (100), 232 (20), 202 (31), 141 (18), 101 (5). UV/Vis (n-hexane): λ_{max} (ϵ): 366 nm ($9600\text{ mol}^{-1} \cdot \text{dm}^3 \cdot \text{cm}^{-1}$); Emission maxima λ_{emi} (n-hexane): 434 nm; Quantum yield of fluorescence Φ_{flu} (n-hexane): 0.72. Elemental analysis Calcd (%) for $\text{C}_{18}\text{H}_{14}\text{O}_2$ (262.3): C, 82.42; H, 5.38; O, 12.20%. Found: C, 82.87; H, 5.62.

2E ((E)-3-(2-anthryl)-2-propenenitrile): a similar procedure, as mentioned above, was adopted using diethylphosphonoacetonitrile to synthesize **2E**, which gave yellow solid. Yield: 80%. $R_f = 0.5$ ($\text{AcOEt}/\text{Hexane}$: 5/95); m.p.: $268\text{—}270^\circ\text{C}$; IR (KBr): $\nu^- = 2213, 1610, 1433, 1329, 1267, 946\text{ cm}^{-1}$; ^1H NMR (200 MHz, CDCl_3): δ 8.64—8.40 (m, 2H, Ar), 8.0—7.97 (m, 3H, Ar), 7.64—7.47 (m, 5H, Ar), 6.15—6.07 (d, 1H, $J = 16.4$ Hz, CHCN); ^{13}C NMR (75 MHz, CDCl_3): δ 149.1, 133.8, 133.6, 131.1, 129.3, 128.1, 126.9, 125.6, 124.3, 117.9, 117.6, 105.2; EI-MS (m/z) (%): 229 (M^+) (45), 171 (25), 141 (12), 95 (80), 59 (76), 43 (100); UV/Vis (n-hexane): λ_{max} (ϵ) = 366 nm ($3871\text{ mol}^{-1} \cdot \text{dm}^3 \cdot \text{cm}^{-1}$); Emission maxima λ_{emi} (n-hexane) = 434 nm; Quantum yield of fluorescence Φ_{flu} (n-hexane) = 0.59.

Elemental analysis Calcd (%) for $C_{17}H_{11}N$ (229.2): C, 89.06; H, 4.84, N, 6.11; Found: C, 89.27; H, 5.01; N, 6.28 %.

1Z (methyl (Z)-3-(2-anthryl)-2-propenoate): bis-(2,2,2-trichloroethyl)-1-carbomethoxy methyl phosphonate (4.17 g, 10 mmol) in dry DMF (15 ml) was added slowly to a suspension of NaH (264 mg, 11 mmol) in dry DMF (10 ml) at rt. The reaction mixture is cooled to $-78^{\circ}C$ and anthracene-2-carbaldehyde **7** (2.06 g, 10 mmol) was added slowly. The reaction mixture is warmed to room temperature, stirred for 3 h and then poured into crushed ice and extracted with ether (3×20 ml). The combined extracts were dried and evaporated under reduced pressure and the residue was purified by column chromatography on silica using AcoEt/Hexane as eluent to give **1Z** as yellow solid. Yield: 70 %. $R_f = 0.76$ (AcOEt/Hexane: 5/95); m.p.: $162-164^{\circ}C$; 1H NMR (200 MHz; $CDCl_3$): δ 8.43—8.38 (m, 2H, Ar), 8.00—7.93 (m, 4H, Ar), 7.73—7.71 (d, 1H, $J = 9.1$ Hz), 7.47—7.45 (m, 2H, Ar), 7.13—7.11 (d, 1H, $J = 12.2$ Hz, $CHCHCO_2CH_3$), 6.06—6.04 (d, 1H, $J = 12.2$ Hz, $CHCO_2CH_3$), 3.85 (s, 3H, CO_2CH_3); UV/Vis (n-hexane): $\lambda_{max}(\epsilon) = 365$ nm ($8400 \text{ mol}^{-1} \cdot \text{dm}^3 \cdot \text{cm}^{-1}$); Emission maxima λ_{emi} (n-hexane) = 430 nm; Quantum yield of fluorescence Φ_{flu} (n-hexane) = 0.68.

3E ((E)-4-(2-Anthryl)-3-buten-2-one): to a solution of 2-anthraldehyde **7** in 50 ml of acetone 2 ml of 5 % NaOH solution was slowly added at $0^{\circ}C$ and stirred at rt for 2 h. The solvent was removed and the product was extracted with chloroform (3×20 ml). The combined extracts were dried and evaporated under reduced pressure and residue was purified by column chromatography on silica using AcoEt/Hexane as eluent to give **3E** as yellow solid. Yield: 90%. $R_f = 0.6$ (AcOEt/Hexane: 10/90); m.p.: $221-223^{\circ}C$; IR (KBr): $\nu^- = 1725, 1667, 1429, 1358, 1249, 977 \text{ cm}^{-1}$. 1H NMR (200 MHz; $CDCl_3$): δ 8.41—8.37 (d, 2H, $J = 8.8$ Hz, Ar), 8.0—7.95 (m, 4H, Ar), 7.77—7.62 (m, 2H, Ar), 7.72—7.6 (d, 1H, $J = 16.2$ Hz, $CHCHCOCH_3$), 7.5—7.45 (m, 2H, Ar), 6.85—6.77 (d, 1H, $J = 16.2$ Hz, $CHCOCH_3$), 2.42 (s, 3H, $COCH_3$); ^{13}C NMR (75 MHz; $CDCl_3$): δ 197.3, 142.3, 133.6, 131.6, 131.1, 130.8, 130.2, 128.3, 127.3, 126.6, 126.3, 125.4, 125.0, 121.5, 26.8; EI-MS (m/z) (%) 246 (M^+) (20), 231 (14), 202 (18), 149 (100), 43 (75). UV/Vis (n-hexane): $\lambda_{max}(\epsilon) = 364$ nm ($6410 \text{ mol}^{-1} \cdot \text{dm}^3 \cdot \text{cm}^{-1}$); Emission maxima λ_{emi} (n-hexane) = 428 nm; Quantum yield of fluorescence Φ_{flu} (n-hexane) = 0.11. Elemental analysis Calcd (%) for $C_{18}H_{14}O$ (246.3): C, 87.78; H, 5.73; O, 6.50 %; Found: C, 88.12; H, 5.86 %.

4E ((E)-2-Nitro-1-ethenyl] anthracene): to the mixture of 2-anthraldehyde **7** (2.06 g, 0.01 mol) and nitromethane (1.2 g, 0.19 mol) in 30 ml of dry dichloromethane 2 drops of piperidine were added. The reaction mixture was refluxed for 8 h. After the completion of the reaction, it was poured into cold water and extracted with dichloromethane (3×20 ml). The combined extracts were dried and evaporated under reduced pressure and the residue was purified by column chromatography on silica using AcoEt/Hexane as eluent to give **4E** (2.24 g, 90 %) as red solid. Yield: 90 %. $R_f = 0.4$ (AcOEt/Hexane: 10/90); m.p.: $212-214^{\circ}C$; IR (KBr): $\nu^- = 1630, 1220, 1026, 771 \text{ cm}^{-1}$; 1H NMR (200 MHz, $CDCl_3$): δ 8.53—8.43 (d, 1H, $J = 14.0$ Hz, $CHCHNO_2$); 8.3—8.2 (m, 4H, Ar), 8.12—8.0 (m, 2H, Ar), 7.78—7.71 (d, 1H, $J = 14.1$ Hz, $CHNO_2$), 7.6—7.5 (m, 3H, Ar); ^{13}C NMR (75 MHz, $CDCl_3$): δ 139.2, 136.9, 134.2, 133.1, 131.9, 130.8, 129.8, 128.4, 128.2, 127.4, 127.2, 126.8, 126.3, 121.7; EI-MS (m/z) (%) = 249 (M^+) (5), 223 (8), 149 (100), 57 (20) 41 (10). UV/Vis (n-hexane): $\lambda_{max}(\epsilon) = 380$ nm ($5510 \text{ mol}^{-1} \cdot \text{dm}^3 \cdot \text{cm}^{-1}$); Emission maxima λ_{emi} (n-hexane) = 454 nm; Quantum yield of fluorescence Φ_{flu} (n-hexane) = 0.03. Elemental analysis Calcd (%) for $C_{16}H_{11}NO_2$ (249.2) C, 77.10; H, 4.45; N, 5.62; Found: C, 77.05; H, 4.32; N, 5.21.

5E ((E)-3-(2-anthryl)-2-propen-1-ol): to a cooled solution of compound **1E** (1.25 g, 5 mmol) in dichloromethane (20 ml), DIBALH (5.3 ml, 7.5 mmol) was added at $-10^{\circ}C$. The reaction mixture was stirred for 30 min at rt. Unreacted DIBALH was quenched with a pinch of NaF/ H_2O at $0^{\circ}C$. The supernatant liquid was filtered, extracted with chloroform (3×15 ml). The combined extracts were dried and evaporated under reduced pressure and purified by column chromatography on silica using AcoEt/Hexane as eluent to give **5E** as yellow solid. Yield: 80 %. $R_f = 0.25$ (AcOEt/Hexane: 10/90); m.p.: $232-236^{\circ}C$; IR (KBr): $\nu^- = 3385, 1617, 1456, 1308, 956 \text{ cm}^{-1}$; 1H NMR (200 MHz; $CDCl_3$): δ 8.5 (s, 2H, Ar), 8.1—7.9 (m, 5H, Ar), 7.51—7.42 (m, 4H, Ar), 6.62—6.5 (m, 2H, $CHCH$), 4.49—4.4 (d, 2H, $J = 6.77$ Hz, CH_2OH); ^{13}C NMR (75 MHz, $CDCl_3$): δ 144.1, 133.3, 132.4, 131.3, 130.4, 129.2,

127.1, 126.4, 124.6, 123.2, 116.4, 63.8; EI-MS (m/z) (%) = 234 (M^+) (21), 215(31), 202 (20), 149 (100); UV/Vis (n-hexane): λ_{\max} (ϵ) = 364 nm ($6345 \text{ mol}^{-1} \cdot \text{dm}^3 \cdot \text{cm}^{-1}$); Elemental analysis Calcd (%) for $\text{C}_{17}\text{H}_{14}\text{O}$ (234.2): C, 87.15; H, 6.02; O, 6.83 %; Found: C, 87.06, H, 5.85.

General procedure for photolysis. A 450 W medium-pressure Hg arc lamp along with suitable filters [63, 64] were used for irradiation. All reactions were monitored by HPLC. An amino silica 5μ , 0.5×25 cm column was used for HPLC analysis. In a typical experiment, 10 ml of a 0.001 M solution of **1E—5E** and **2Z**, N_2 bubbled, was used for irradiation. After irradiation, the products were characterized by comparison with authentic materials. Triplet sensitized reactions were carried out using a mixture of sensitizer (0.01 M) and substrate (**1E—5E** and **1Z** 0.001 M) in MeOH (10 ml), N_2 bubbled, which was irradiated for 1 h using a 450 W Hg lamp with filters.

Fluorescence. A fluorimeter equipped with a 450 W Xe lamp was used for fluorescence studies. Dry solvents were used, and identical conditions were maintained for all the fluorescence measurements. The slit widths were $2 \times 2 \times 2$ mm. The emission spectral range was 350—500 nm. All operations were at room temperature. The quantum yield of fluorescence was determined relative to that of 9,10-diphenylanthracene (0.9) [65, 66].

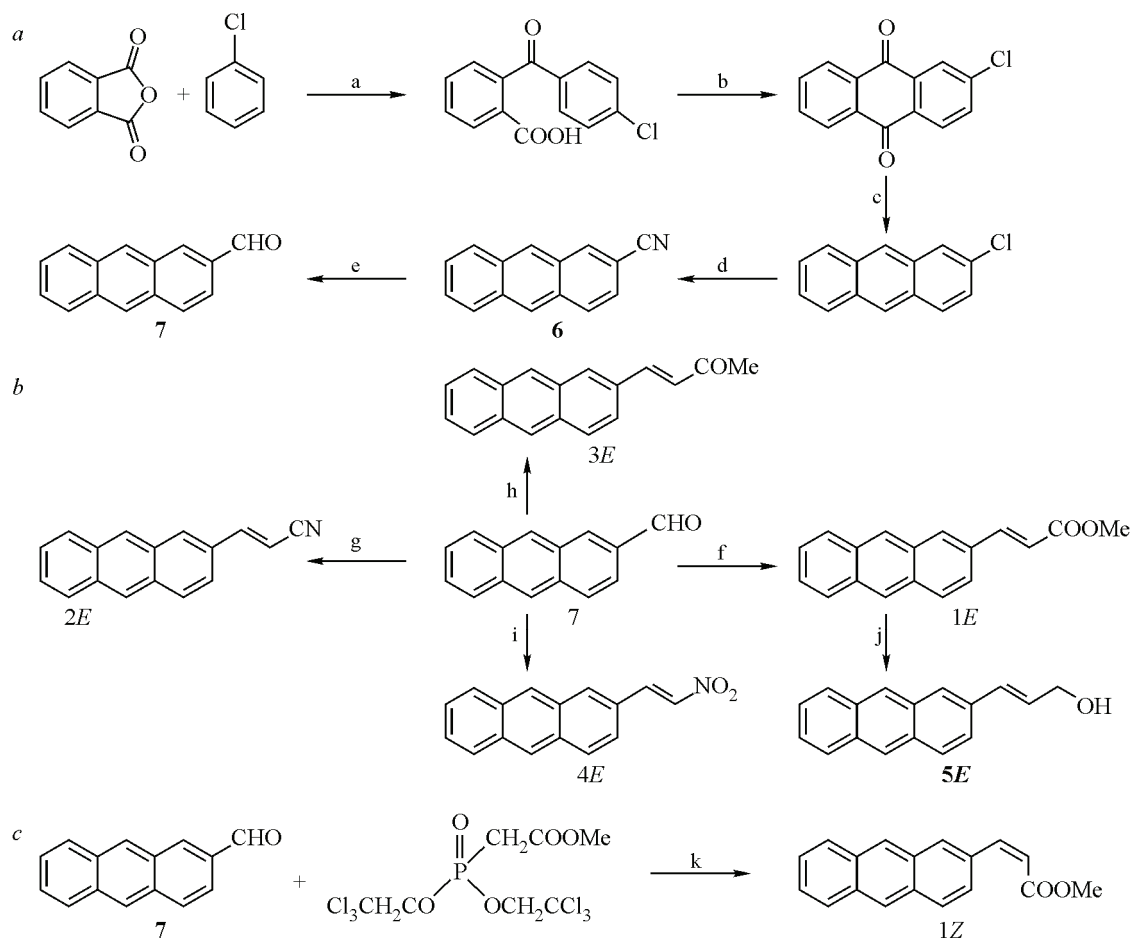
RESULTS

Synthesis of 2-anthrylethylene derivatives. 2-Anthrylethylene derivatives **1E—5E** and **1Z** were synthesized to study $Z \rightleftharpoons E$ photoisomerization, fluorescence, and rotamerism (conformational isomerization). 2-Anthracene carbaldehyde **7** is the key intermediate involved in the synthesis of **1E—5E** and **1Z** compounds (Scheme 1). Friedel—Crafts phthaloylation on chlorobenzene [67] gave chlorobenzophenone carboxylic acid, which upon treatment with sulfuric acid produced 2-chloroanthraquinone [68]. 2-Chloroanthraquinone was subsequently converted into 2-chloroanthracene [69] and then to 2-cyanoanthracene [70]. 2-Cyanoanthracene was transformed to the key intermediate 2-anthracene carbaldehyde **7** using DIBALH [71] (Scheme 1). Compound **7** was subjected to Horner-Wadsworth-Emmons olefination using suitable phosphonates [72, 73] to obtain **1E** and **2E**. Condensation of **7** with acetone afforded compound **3E** and with nitromethane yielded **4E**. Reduction of **1E** using DIBALH provided compound **5E** [62]. The **1Z** isomer was synthesized by adopting HWE olefination using a modified phosphonate reagent [74], previously reported by us (Scheme 1).

Photochemical $Z \rightleftharpoons E$ (*cis* \rightleftharpoons *trans*) isomerization. 2-Anthrylethylene derivatives **1E—5E** and **1Z** were subjected to direct and triplet sensitized $Z \rightleftharpoons E$ isomerization. Compound **1Z** upon direct excitation and triplet sensitization underwent *Z* (*cis*) to *E* (*trans*) isomerization exclusively, within 15 minutes and in quantitative yield. The *E* (*trans*) isomers of **1—5** did not undergo *E* (*trans*) to *Z* (*cis*) isomerization upon direct excitation in various solvents or upon triplet sensitization, unlike 9-anthrylethylene derivatives [60—62], but **1Z** displayed *one-way* *Z* (*cis*) to *E* (*trans*) isomerization (Scheme 2; Table 1). Triplet energy of the sensitizers [63—66] used varied between 160—184 $\text{kJ} \cdot \text{mol}^{-1}$. Prolonged irradiation (~ 400 nm, 3 h to 12 h) of compounds **1E—5E** and **1Z** did not yield any new products other than the *E* (*trans*) isomer, as judged by ^1H NMR.

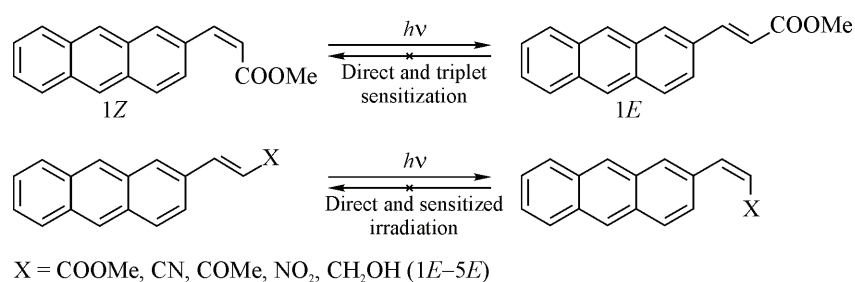
Absorption and fluorescence studies. Absorption and fluorescence studies were carried out in various organic solvents to understand the ground and excited state properties of 2-anthrylethylene derivatives and the data was compiled in Table 2. The absorption spectra of these derivatives are structured with a vibronic progression characteristic of the anthryl chromophore. This suggests that the excitation energy is largely localized in the anthryl chromophore, whereas 9-anthrylethylenes, carrying electron-withdrawing end groups, exhibited broad absorption in the 300—450 nm region [60—62]. The UV-visible absorption of **1E**, **2E**, **3E**, and **5E** shows a slight bathochromic shift (2—10 nm) upon increasing the solvent polarity. A prominent bathochromic shift is observed for compound **4E** in the UV-vis absorption maxima with an increase in solvent polarity (Fig. 1).

The steady state fluorescence spectra of all the compounds were recorded at room temperature in various organic solvents. The fluorescence emission maxima and quantum yield of fluorescence data are given in Table 2; the corresponding fluorescence spectra for four compounds are displayed in Figs. 2—5. The excitation wavelength strongly affects the fluorescence spectra of derivatives **1E—5E**.



Scheme 1. Reagents and conditions: (a) AlCl_3 , 60°C , 8 h (b) conc. H_2SO_4 , 135°C , 6 h (c) Zn dust/ AcOH /pyridine, 110°C , 8 h; (d) CuCN , pyridine, 220°C , 24 h; (e) DIBALH, -78°C , 4 h. (f) $(\text{EtO})_2\text{P}(\text{O})\text{CH}_2\text{COOMe}$, NaH, DMF, rt and 4 h; (g) $(\text{EtO})_2\text{P}(\text{O})\text{CH}_2\text{CN}$, NaH, DMF, rt, 4 h; (h) Acetone, 5 % NaOH, rt, 2 h; (i) nitromethane, piperidine, dichloromethane, 40°C ; (j) DIBALH, 0°C , 6 h. (k) NaH, DMF, rt, cool to -78°C , then add 2-anthraldehyde

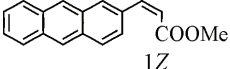
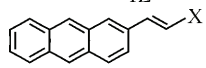
Compounds **1E** to **3E** and **1Z** display structured fluorescence in nonpolar solvents, such as hexane and cyclohexane, whereas broad fluorescence emission was observed in polar solvents. Compound **4E** did not exhibit structured fluorescence both in nonpolar and polar solvents due to the strong electron-withdrawing nature of the nitro group. On the other hand, compound **5E** displayed structured fluorescence irrespective of the solvent polarity. The fluorescence emission of all these derivatives, except that of **5E**, were found to be sensitive towards the solvent polarity. The fluorescence quantum yield calculated for compounds **1E**, **2E**, and **5E** is high (Table 2) compared to that of compounds **3E** and **4E**,



Scheme 2. Photochemical $Z \rightleftharpoons E$ (*cis* \rightleftharpoons *trans*) isomerization of compounds **1Z** and **1E**–**5E**

Table 1

Photochemical *Z*–*E* isomerization of 2-anthrylethylene derivatives (**1Z** and **1E–5E**)

| Compound ^a | Photolysis | Photo-isomer composition ^b | |
|---|-----------------------------------|---------------------------------------|----------------------------|
| | | <i>E</i> (<i>trans</i>), % | <i>Z</i> (<i>cis</i>), % |
|  | Direct and Sensitized irradiation | 98 | 2 |
|  <i>1E–5E</i> (X = COOMe, CN, COMe, NO ₂ , CH ₂ OH) | Direct and Sensitized irradiation | 100 | 0 |

^a The nitrogen bubbled 0.001 M solutions were irradiated (15 min for **1Z** and 3–12 h for **1E–5E**). A 450 W Hg arc lamp (~400 nm) was used and 0.001 M methanol solutions with 0.01 M sensitizers rose Bengal (163 kJ·mol⁻¹), erythrosine (176 kJ·mol⁻¹), and eosine (180 kJ·mol⁻¹) were used for sensitized irradiations (>500 nm, 15 min for **1Z** and 3–6 h for **1E–5E**) — a 450 W Hg arc lamp with filter solutions was used.

^b Photo isomer composition was analysed by normal phase HPLC and ¹H-NMR.

Table 2

UV-Visible absorption and fluorescence of compounds **1E–5E**

| Compound ^a | Solvent | λ_{abs} , nm | λ_{flu} , nm | Φ_{flu} |
|-----------------------|--------------|-----------------------------|---------------------------------|---------------------|
| 1E | Cyclohexane | 356, 365, 384, 400 | 406, 434, 458, 490 (<i>s</i>) | 0.75 |
| | Hexane | 356, 366, 384, 400 | 406, 432, 458, 486 (<i>s</i>) | 0.72 |
| | Chloroform | 354, 364, 400 | 454 | 0.62 |
| | Acetonitrile | 354, 364, 400 | 460 | 0.41 |
| | Methanol | 354, 364, 382, 402 | 480 | 0.66 |
| 2E | Cyclohexane | 354, 366, 382, 404 | 408, 434, 458, 492 (<i>s</i>) | 0.61 |
| | Hexane | 354, 366, 382, 404 | 410, 436, 462, 490 (<i>s</i>) | 0.59 |
| | Chloroform | 354, 366, 382, 406 | 455 | 0.40 |
| | Acetonitrile | 354, 366, 382, 406 | 456 | 0.41 |
| | Methanol | 354, 366, 382, 406 | 462 | 0.57 |
| 3E | Cyclohexane | 366, 382, 404 | 386, 410, 430, 453 (<i>s</i>) | 0.14 |
| | Hexane | 364, 382, 404 | 385, 406, 428, 452 (<i>s</i>) | 0.11 |
| | Chloroform | 366, 384, 408 | 476 | 0.22 |
| | Acetonitrile | 356, 386, 410 | 483 | 0.18 |
| | Methanol | 356, 386, 406 | 536 | 0.12 |
| 4E | Cyclohexane | 362, 372, 402, 426 | 451 | 0.031 |
| | Hexane | 360, 376, 426 | 454 | 0.03 |
| | Chloroform | 362, 380, 434 | 595 | 0.14 |
| | Acetonitrile | 360, 376, 424 | 615 | 0.096 |
| 5E | Hexane | 356, 364, 382, 404 | 386, 397, 422, 450 (<i>s</i>) | 0.56 |
| | Acetonitrile | 356, 365, 400 | 399, 416, 450 (<i>s</i>) | 0.42 |
| 1Z | Hexane | 356, 365, 384, 400 | 406, 430, 457, 486 (<i>s</i>) | 0.68 |
| | Acetonitrile | 355, 364, 400 | 460 | 0.40 |

^a Nitrogen bubbled 0.00001 M solutions were used for measuring the fluorescence at room temperature; quantum yields of fluorescence were determined using 9,10-Diphenyl anthracene ($\Phi_{\text{flu}} = 0.9$) as standard⁴⁶; experimental error is ± 10 %.

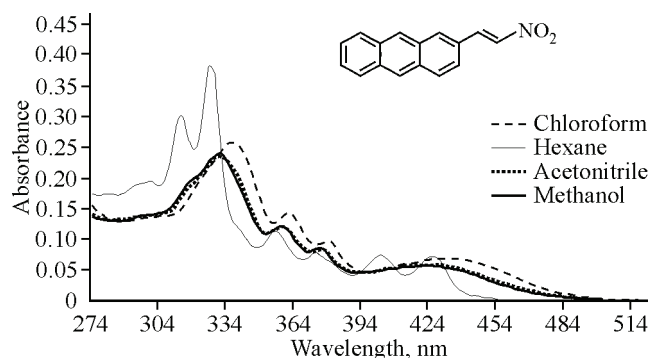


Fig. 1. UV-Visible absorption spectra of **4E** (10^{-5} M) in various solvents

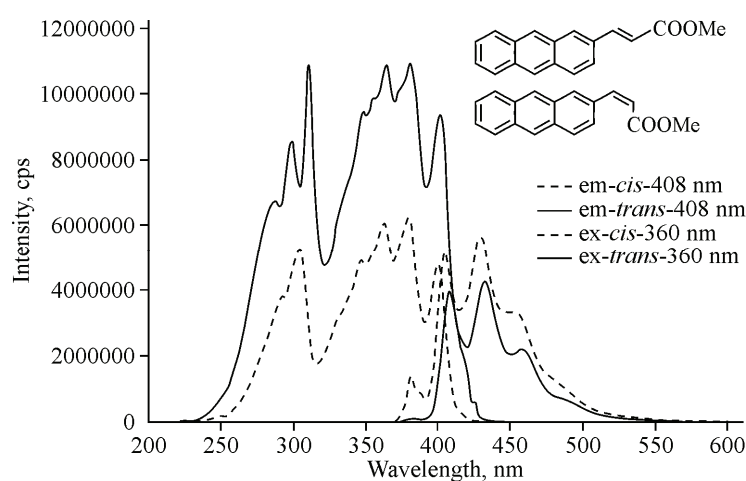


Fig. 2. Normalized fluorescence excitation and emission spectra **1E** and **1Z** in hexane (10^{-5} M)

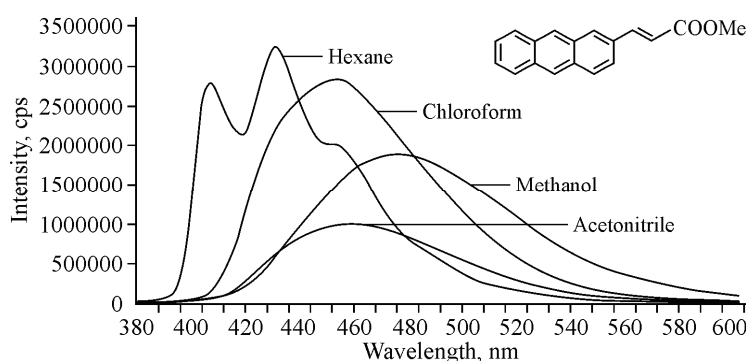


Fig. 3. Effect of solvent on the fluorescence spectrum of **1E** (10^{-5} M)

and this may be due to the intersystem crossing leading to a more populated triplet excited state. Fig. 2 shows the emission and excitation spectra of **1E** and **1Z**, and the fluorescence emission spectrum of *cis* isomer **1Z** is almost similar to the emission spectrum of *trans* isomer **1E**. Fig. 3 shows fluorescence of **1E** in various solvents. The fluorescence spectrum is broadened and the maximum is shifted to longer wavelength on increasing the solvent polarity. Interestingly, fluorescence emission for these compounds is found to be excitation wavelength dependent suggesting the involvement of the conformers (rotamers) at room temperature. The fluorescence spectra of **1E** and **2E** in hexane are displayed in Figs. 4 and 5. The fluorescence spectra were recorded by exciting at different wavelengths ranging from the lower wavelength region (330–400 nm; Fig. 4) to a higher wavelength region (400–420 nm; Fig. 4) for **1E**. The fluorescence maxima (λ_{flu}) were observed at 406 nm, 432 nm, and 458 nm when the excitation was performed at 330–400 nm. Interestingly, upon excitation at 410 nm the fluorescence maxima were red shifted to 422 nm, 448 nm, and 478 nm. Similarly, for compound **2E** upon excitation at a lower wavelength region (330–400 nm) the fluorescence maxima (λ_{flu}) were observed at 410 nm, 436 nm, and 462 nm (Fig. 5) and upon excitation at 420 nm the fluorescence maxima were found at 424 nm, 448 nm, and 472 nm (Fig. 5). All the other derivatives exhibited similar behavior.

Fluorescence lifetimes.

The fluorescence lifetime profiles were obtained for 2-anthrylethylene derivatives (**1E**–**2E**) using a single photon counting nano-LED spectrofluorimeter (IBH) with a time resolution of around 1 ns. The excitation wavelengths were 374 nm and 439 nm and the fluorescence decay was monitored near the emission maximum (Table 3). Satisfactory fits to a single exponential were obtained for 374 nm excitation in all the solvents for these two compounds, and double exponential fits were found to be the most appropriate for 439 nm excitation in hexane and cyclohexane solvents (Table 3).

Computational methods and conformational analysis. It is very important in terms of materials based on the isomerization to consider the reasons why *s-trans* is more stable than *s-cis* in the

ground as well as the excited state. For this purpose we applied DFT and *ab initio* tools to evaluate the relative energy difference of the conformers of **1E**–**5E** compounds [75]. Geometry optimizations of **1E**–**5E** molecules (Chart) were performed at HF/6-31G(*d,p*) and B3LYP/6-31G(*d,p*) levels of theory for the S_0 state and the CIS/6-31G(*d,p*) level for the S_1 state without restricting the symmetry. Two potential minima (*s-trans* and *s-cis* rotamers — rotational axis C_2 – C_{11} bond) are obtained for each molecule. In the *s-trans* rotamer, C_1 and C_{12} carbon atoms are *trans* to each other, whereas in *s-cis*, they are *cis* to each other. In both S_0 and S_1 states, irrespective of the acceptor, *s-trans* is found to be stable compared to the *s-cis* rotamer (Table 4). The energy difference between these rotamers is very small and it varies from $3.3 \text{ kJ}\cdot\text{mol}^{-1}$ to $6.7 \text{ kJ}\cdot\text{mol}^{-1}$ for different substituents at various levels of theory. This minor difference was expected due to the steric effects in the single bond rotation. The dipole moment difference of these rotamers is also very small in both states. The computational studies show that none of the molecules are planar in the ground state, whereas in the first excited state, they are nearly planar. The twist angle between the anthracene plane and the olefinic double bond ranges from 5° to 30° , which is attributed to the interaction of the *ortho* protons of anthracene with the olefinic protons. Selected bond lengths C_2 – C_{11} (R_1),

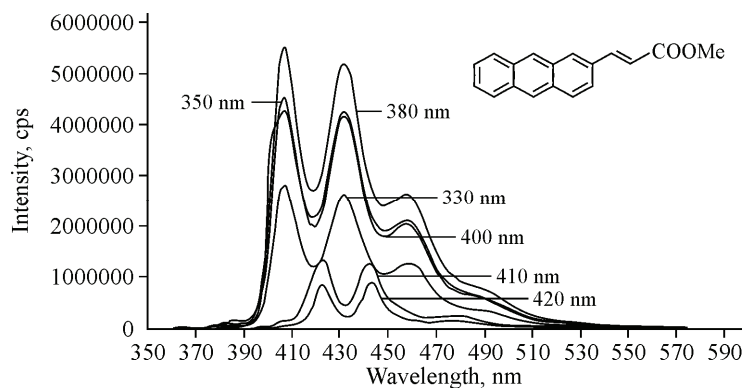


Fig. 4. Fluorescence emission spectra of **1E** in hexane (10^{-5}) as a function of the excitation wavelength

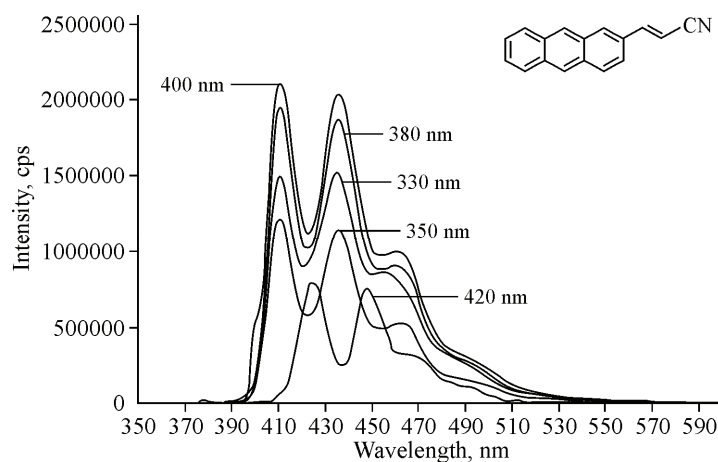


Fig. 5. Fluorescence emission spectra of **2E** in hexane (10^{-5}) as a function of excitation wavelength

Table 3

Excitation wavelength dependent fluorescence lifetimes of compounds **1E** and **2E**

| Solvent | Compound 1E ^a | | | Compound 2E ^a | | |
|--------------|---------------------------------|---------------|---------------|---------------------------------|---------------|---------------|
| | λ_{ex} , nm | τ_1 , ns | τ_2 , ns | λ_{ex} , nm | τ_1 , ns | τ_2 , ns |
| Cyclohexane | 374 | 9.38 | — | 374 | 9.90 | — |
| | 439 | 4.13 | 0.080 | 439 | 5.72 | 0.285 |
| Hexane | 374 | 8.01 | — | 374 | 8.54 | — |
| | 439 | 4.02 | 0.0004 | 439 | 5.15 | 0.112 |
| Chloroform | 374 | 5.40 | — | 374 | 6.24 | — |
| Acetonitrile | 374 | 6.30 | — | 374 | 6.75 | — |
| Methanol | 374 | 6.39 | — | 374 | 6.62 | — |

^a Nitrogen bubbled solutions 1.0×10^{-5} M were used; λ_{em} at 480 nm.

Table 4

Relative energies (ΔE) and dipole moment (μ)^a of **1E**–**5E**

| Compound | HF/6-31G(<i>d,p</i>) | | B3LYP/6-31G(<i>d,p</i>) | | CIS/6-31G(<i>d,p</i>) | |
|-----------|-----------------------------------|-----------|-----------------------------------|-----------|-----------------------------------|-----------|
| | ΔE , kJ·mol ⁻¹ | μ , D | ΔE , kJ·mol ⁻¹ | μ , D | ΔE , kJ·mol ⁻¹ | μ , D |
| 1E | 5.3 | 2.7 (2.5) | 5.6 | 2.7 (2.5) | 5.6 | 3.2 (2.6) |
| 2E | 5.2 | 6.4 (6.5) | 5.1 | 6.1 (6.3) | 5.1 | 6.4 (6.5) |
| 3E | 5.2 | 4.3 (4.1) | 4.1 | 3.9 (3.6) | 5.5 | 4.8 (4.3) |
| 4E | 6.1 | 7.8 (8.2) | 5.4 | 7.0 (7.2) | 6.5 | 8.9 (9.1) |
| 5E | 3.2 | 2.1 (2.0) | 4.2 | 1.6 (1.5) | 4.0 | 2.2 (2.1) |

^a Dipole moment (Debye) of *s-trans* is in parenthesis.

Table 5

Bond Lengths (\AA) of **1E**–**5E** in S_0 and S_1 -state

| Compound | | R_1 (C ₂ —C ₁₁) | | R_2 (C ₁₁ —C ₁₂) | | R_3 (C ₁₂ —C ₁₃) | |
|-----------|----------------|--|-------|---|-------|---|-------|
| | | S_0 | S_1 | S_0 | S_1 | S_0 | S_1 |
| 1E | <i>s-trans</i> | 1.465 | 1.447 | 1.333 | 1.343 | 1.463 | 1.454 |
| | <i>s-cis</i> | 1.467 | 1.438 | 1.332 | 1.348 | 1.464 | 1.452 |
| 2E | <i>s-trans</i> | 1.465 | 1.446 | 1.333 | 1.345 | 1.475 | 1.465 |
| | <i>s-cis</i> | 1.462 | 1.439 | 1.333 | 1.351 | 1.476 | 1.462 |
| 3E | <i>s-trans</i> | 1.458 | 1.449 | 1.336 | 1.343 | 1.427 | 1.422 |
| | <i>s-cis</i> | 1.461 | 1.441 | 1.338 | 1.349 | 1.429 | 1.420 |
| 4E | <i>s-trans</i> | 1.459 | 1.431 | 1.328 | 1.349 | 1.431 | 1.404 |
| | <i>s-cis</i> | 1.464 | 1.426 | 1.327 | 1.354 | 1.432 | 1.401 |
| 5E | <i>s-trans</i> | 1.473 | 1.464 | 1.327 | 1.331 | 1.492 | 1.491 |
| | <i>s-cis</i> | 1.470 | 1.457 | 1.326 | 1.335 | 1.493 | 1.490 |

C₁₁—C₁₂ (R_2), and C₁₂—C₁₃ (R_3) of the optimized geometries of **1E**–**5E** in the ground state (HF/6-31G (*d,p*)) and the excited state (CIS/6-31G(*d,p*)) are presented in Table 5. Bond length alternation is observed from the ground state to the excited state in all the molecules. The C₂—C₁₁ bond length of *s-trans* of the **1E** molecule is 1.465 Å in the S_0 state and it is reduced to 1.447 Å in the S_1 state. Similar behavior is observed for the C₁₂—C₁₃ bond in S_0 and S_1 states, measuring 1.463 Å and 1.454 Å respectively. In contrast, the C₁₁—C₁₂ bond in the S_0 state is 1.333 Å and it is elongated to 1.343 Å in the S_1 state. A similar kind of alteration is observed in both rotamers of all the molecules, i.e. in the S_1 state compared to the S_0 state, R_1 is reduced, but R_2 is elongated and again R_3 is reduced.

Computed absorption and emission analysis. UV-Visible absorption data indicate that there is not much ground state and medium interaction in almost all of the substrates (Table 2). The absorption spectrum of these derivatives is structured with a vibronic progression characteristic of the anthryl chromophore confirming that the excitation energy is largely localized on the anthryl chromophore, whereas 9-anthrylethylenes, carrying electron-withdrawing end groups, exhibit broad absorption in the 300–450 nm region [62]. In order to further analyze the nature of charge transfer, we have carried out theoretical calculations of vertical excitations at HF/6-31G (*d,p*) optimized geometries of all the conformations for each molecule using ZINDO-SCI; the results are shown in Table 6. The selected HOMO and LUMO orbitals of both rotamers in **1E** and **5E** molecules are shown in Fig. 6. In the HOMO of **1E** and **5E**, the electron density is located mainly on the anthracene moiety. In HOMO-1 of **1E**, it is spreaded over both anthracene as well as olefinic double bond. But in the case of the LUMO

Table 6

Computed electronic absorption and emission spectra of **1E**–**5E**

| Compound | Rotamer | State | λ_{abs} , nm | f | Major Transitions (CI) | λ_{em} , nm | f |
|-----------|----------------|-------|-----------------------------|-------|------------------------------|----------------------------|-------|
| 1E | <i>s-trans</i> | S_1 | 409 | 0.129 | H→L (0.63); H-1→L (-0.14) | 438 | 0.163 |
| | | S_2 | 359 | 0.008 | — | 368 | 0.017 |
| | | S_3 | 300 | 1.388 | — | 303 | 0.291 |
| | <i>s-cis</i> | S_1 | 431 | 0.093 | H→L (0.63); H-1→L (-0.11) | 462 | 0.136 |
| | | S_2 | 359 | 0.012 | — | 366 | 0.008 |
| | | S_3 | 307 | 1.041 | — | 312 | 0.04 |
| 2E | <i>s-trans</i> | S_1 | 411 | 0.123 | H→L (0.62); H-1→L (-0.16) | 436 | 0.143 |
| | | S_2 | 359 | 0.009 | — | 366 | 0.014 |
| | | S_3 | 297 | 1.432 | — | 297 | 1.325 |
| | <i>s-cis</i> | S_1 | 437 | 0.087 | H→L (0.63); H-1→L (-0.12) | 463 | 0.012 |
| | | S_2 | 358 | 0.021 | — | 364 | 0.01 |
| | | S_3 | 305 | 1.03 | — | 306 | 0.985 |
| 3E | <i>s-trans</i> | S_1 | 414 | 0.139 | H→L (0.63); H-1→L (-0.12) | 443 | 0.175 |
| | | S_2 | 362 | 0.011 | — | 373 | 0.018 |
| | | S_3 | 306 | 1.237 | — | 310 | 1.166 |
| | <i>s-cis</i> | S_1 | 437 | 0.1 | H→L (0.63); H-1→L (-0.12) | 468 | 0.145 |
| | | S_2 | 362 | 0.016 | — | 371 | 0.012 |
| | | S_3 | 313 | 0.986 | — | 317 | 0.982 |
| 4E | <i>s-trans</i> | S_1 | 451 | 0.151 | H→L (0.64); H-1→L (-0.15) | 489 | 0.211 |
| | | S_2 | 366 | 0.024 | — | 378 | 0.03 |
| | | S_3 | 326 | 0.805 | — | 331 | 0.844 |
| | <i>s-cis</i> | S_1 | 477 | 0.108 | H→L (0.65); H-1→L (-0.12) | 519 | 0.164 |
| | | S_2 | 368 | 0.021 | — | 379 | 0.028 |
| | | S_3 | 331 | 0.738 | — | 337 | 0.804 |
| 5E | <i>s-trans</i> | S_1 | 390 | 0.082 | H→L (0.63) | 422 | 0.087 |
| | | S_2 | 347 | 0.001 | — | 350 | 0.002 |
| | | S_3 | 282 | 0.466 | — | 289 | 0.143 |
| | <i>s-cis</i> | S_1 | 403 | 0.06 | H→L (0.64) | 438 | 0.078 |
| | | S_2 | 345 | 0.01 | — | 351 | 0.007 |
| | | S_3 | 286 | 0.129 | — | 294 | 0.017 |

Coefficients indicated in parentheses; H indicates HOMO and L indicates LUMO.

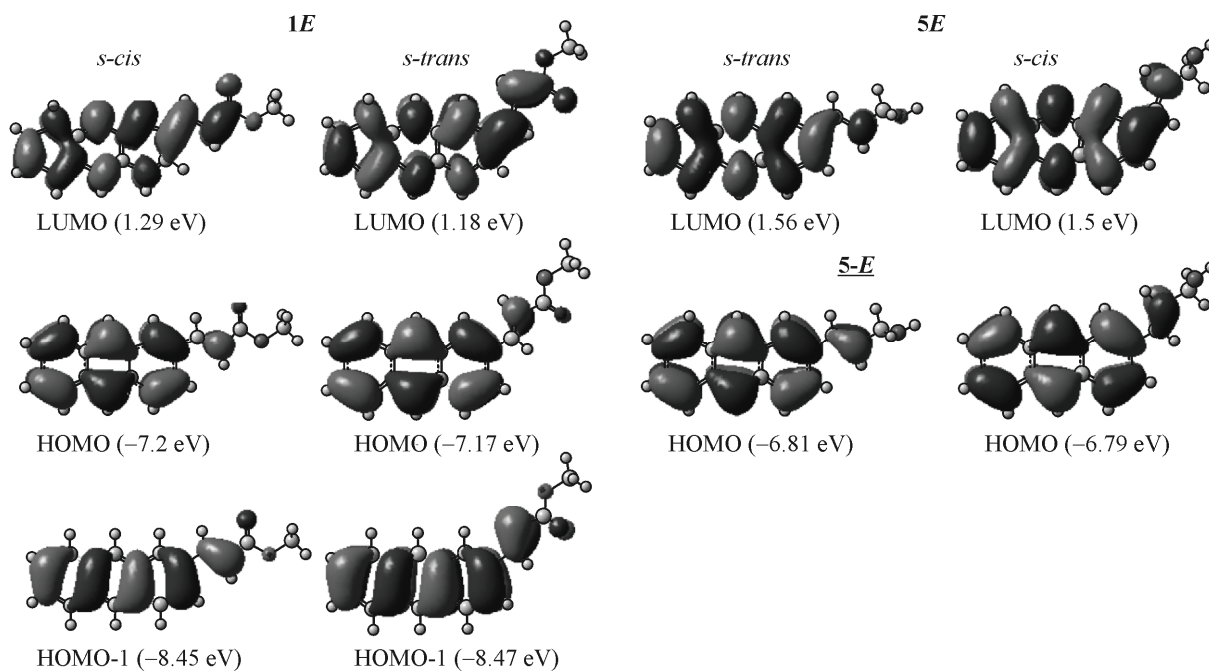


Fig. 6. Frontier molecular orbital pictures of $1E$ & $5E$

of $1E$, the electron density is located all over the molecule, i.e. it is extended to the acceptor also. In contrast, for $5E$ the reorganization of the electron density is observed within the anthracene and olefinic bond. Computed electronic excitation values are in good agreement with the experimental results. Computed electronic absorption of the $1E$ molecule is 409 nm and 431 nm for *s-trans* and *s-cis* rotamers respectively. Absorption analysis is carried out to know the transitions responsible for the absorption maxima presented in the same table. Table 6 illustrates that the mixture of transitions (HOMO to LUMO, HOMO-1 to LUMO) is responsible for the observed absorption maxima in both *s-trans* and *s-cis* of the $1E$ molecule. This reveals that charge transfer in $1E$ takes place from the donor groups (anthracene) to the acceptor (end) groups. The calculated absorption maxima are in good agreement with experimentally observed 400 nm in hexane. Owing to the interconversion between two rotamers at room temperature average (single) absorption maxima are observed experimentally. The second and third transitions are 359 nm, 300 nm and 359 nm, 307 nm for *s-trans* and *s-cis* rotamers respectively, which is slightly overestimated compared to the experimental results i.e. 380 nm and 360 nm for S_2 and S_3 transitions. This is attributed to the calculations being carried out in the gas phase, whereas the experimental results are obtained in the solvent environment (condensed media). For the $3E$ molecule, the calculated S_1 , S_2 , S_3 transitions are 414 nm, 362 nm, and 306 nm for *s-trans* and 437 nm, 362 nm, 313 nm for the *s-cis* rotamer, which coincides with experimental 404 nm, 382 nm, and 366 nm. Similarly, the calculated absorption values for *s-trans* and *s-cis* of $4E$ – $5E$ molecules are also in good agreement with the experimental results. For all the molecules except for $5E$ the major (HOMO to LUMO) and minor transitions (HOMO-1 to LUMO) are combinedly responsible for the observed absorption maxima. In the case of the $5E$ molecule, only one transition, i.e. HOMO to LUMO, is responsible for the absorption maxima of both rotamers. This discrepancy can be explained by considering their end groups, which are acceptors in $1E$ – $4E$ molecules, but donors in the $5E$ molecule. Hence, the absorption maxima of the $5E$ molecule is slightly blue shifted compared to the other molecules ($1E$ – $4E$) and the HOMO-1 to LUMO transition disappears.

DISCUSSION

The red shift observed in the emission maxima (fluorescence solvatochromism) [76, 77] for compounds $1E$ – $4E$ by changing the solvent polarity indicates that the singlet excited state has some amount of charge transfer or polar character [78]. Frontier Molecular Orbital analysis (Fig. 6) reveals

that the partial charge transfer occurs from the donor to the acceptor when it is excited for **1E**–**4E** molecules. This is also observed in the geometry of S_1 vs. S_0 where single and double bond alteration occurred. From the solvent effects it can also be concluded that the molecule is polarized in the excited state, and hence, it exhibits different interactions with nonpolar and polar solvents. In contrast, compound **5E** did not exhibit fluorescence solvatochromism and this infers the non-involvement of the charge transfer excited state, which is due to the lack of electron- withdrawing acceptor groups, and the same is noticed in the frontier molecular orbital of **5E** (Fig. 6). The fluorescence maxima (λ_{flu}), for compound **1E** were observed at 406 nm, 432 nm, and 458 nm upon excitation at 330–400 nm. When the same compound was subjected to excitation at 410 nm, different fluorescence maxima were observed at 422 nm, 448 nm, and 478 nm (Fig. 4). The two different fluorescence emission spectra correspond to the two rotamers, because of different absorptivities at the given λ of excitation. Similar excitation wavelength dependent fluorescence emission is observed for the other molecules (Fig. 5). The computed emission spectra of the **1E** molecule (438 nm for *s-trans* and 462 nm for the *s-cis* rotamer) are in good agreement with the experimental results (Fig.4; Table 6). This is further supported by the fluorescence lifetime data recorded (Table 3) where biexponential decay becomes prominent at λ_{exci} of 439 nm. The excitation at 374 nm provides single exponential decay (Table 3) for compounds **1E** and **2E**, and this indicates the selective population of the excited rotamer (Scheme 3). Interconversion of the excited rotamers (Scheme 3) is predicted as not a feasible process, according to the NEER principle. These excited rotamers do not undergo *E*–*Z* isomerization, but exhibit only fluorescence (Scheme 3). A comparison of both experimental and theoretical results reveals that two rotamers (Chart 1) exist in the excited state. These rotamers have different first lowest excited states, and hence, it is reflected in fluorescence emission.

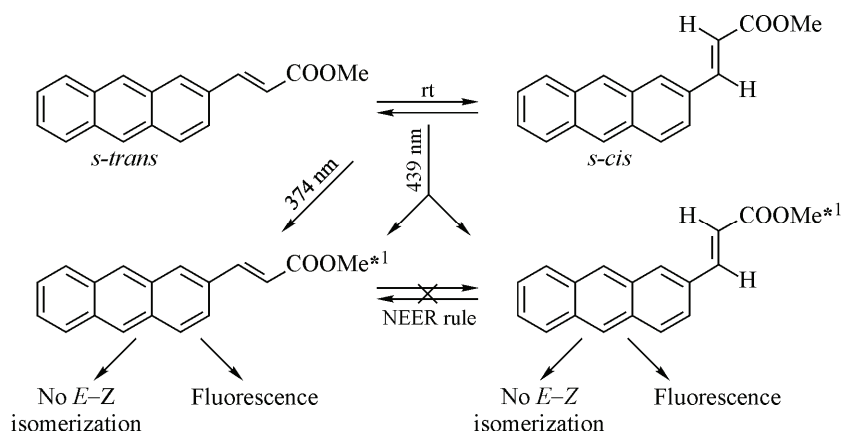
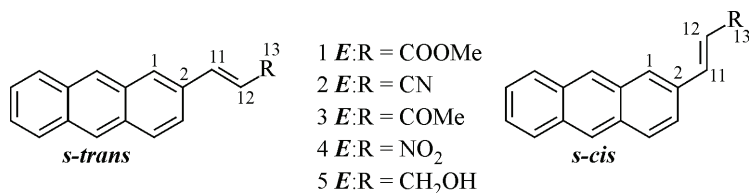
Scheme 3. Excited state profile of compound **1E**

Chart 1. List of molecules and corresponding rotamers

CONCLUSIONS

In conclusion, 2-anthrylethylene derivatives (**1E**–**5E** and **1Z**) were synthesized to study photochemical *Z* (*cis*)–*E* (*trans*) isomerization. All the derivatives did not undergo *E* (*trans*) to *Z* (*cis*) isomerization upon direct and triplet sensitization. But compound **1Z** exhibited efficient *one-way Z* (*cis*) to *E* (*trans*) isomerization upon direct and sensitized irradiation. The UV-Visible absorption spec-

tra of **1E**, **2E**, **3E**, and **5E** displayed a slight bathochromic shift (2–10 nm) upon changing the solvent polarity from non-polar hexane to polar methanol. A prominent bathochromic shift of the UV-Visible absorption maximum was observed for compound **4E** with an increase in the solvent polarity. Compounds **1E**–**4E** displayed fluorescence solvatochromism due to the polar nature of the singlet excited state. Compounds **1E**–**5E** exhibited strong dependence of fluorescence on the excitation wavelength due to the presence of two rotamers. Fluorescence decay profiles also indicate the presence of two rotamers in 2-anthrylethylene derivatives **1E** and **2E**. Fluorescence life time studies carried out at room temperature revealed that 2-anthrylethylene derivatives **1E**–**5E** exhibited *s-trans* and *s-cis* rotational isomers. Steady state fluorescence experiments indicated that compounds **1E**–**5E** exhibited intense emission corresponding to the *s-trans* rotational isomer with shorter λ_{max}^f upon excitation at a lower wavelength region (320–390 nm), and weak emission corresponding to the *s-cis* rotational isomer with longer λ_{max}^f is noticed upon excitation at a higher wavelength region (400–420 nm). Theoretical studies performed also supported the existence of rotational isomers, and the *s-trans* rotamer is more stable than the *s-cis* rotamer.

Acknowledgements. We thank Director, IICT, Project Director, NIPER, and the Head of the Division for the encouraging support. P. Arun Kumar and Kolupula Srinivas thank CSIR-New Delhi and U. Srinivas thanks UGS-New Delhi for fellowships. We thank Prof. A. Samantha for providing life time measurement data.

REFERENCES

1. Hammond G.S., Saltiel J., Lamola A.A., Turro N.J., Bradshaw J.S., Cowan D.O., Counsell R.C., Vogt V., Dalton C. // J. Amer. Chem. Soc. – 1964. – **86**. – P. 3197 – 3217.
2. Hammond H.A., DeMeyer D.E., Williams J.L.R. // J. Amer. Chem. Soc. – 1969. – **91**. – P. 5180 – 5181.
3. Waldeck D.H. // Chem. Rev. – 1991. – **91**. – P. 415 – 436.
4. Gorner H., Kuhn H. // J. Adv. Photochem. – 1995. – **19**. – P. 1 – 117.
5. Saltiel J., Sun Y.P. / Eds. Photochromism, Molecular Systems. – Elsevier: Amsterdam, 1990.
6. Merer A.J., Mulliken R.S. // Chem. Rev. – 1969. – **69**. – P. 639 – 656.
7. Mulliken R.S. // J. Chem. Phys. – 1977. – **66**. – P. 2448 – 2451.
8. Meier H. // Angew. Chem., Int. Ed. Engl. – 1992. – **31**. – P. 1399 – 1420.
9. Simeonov A., Matsuhita M., Juban E.A., Thompson E.H.Z., Hoffmann T.Z., Beuscher IV A.E., Taylor M.J., Peter Wirsching, Wolfgang Rettig, Mc Cusker J.K., Stevens R.C., Miller D.P., Schultz P.G., Lerner R.A., Janda K.D. // Science. – 2000. – **290**. – P. 307 – 313.
10. Papper V., Likhstenshtein G.I. // J. Photochem. Photobiol. A. – 2001. – **140**. – P. 39 – 52.
11. Saltiel J., Krishna T.S.R., Turek A.M. // J. Amer. Chem. Soc. – 2005. – **127**. – P. 6938 – 6939.
12. Akiu K., Saijo M., Ikegami M., Arai T. // Bull. Chem. Soc. Jpn. – 2005. – **78**. – P. 1132 – 1137.
13. Momotake A., Arai T. // J. Photochem. Photobiol. C. – 2004. – **5**. – P. 1 – 25.
14. Roberts J.C., Pincock J.A. // J. Org. Chem. – 2006. – **71**. – P. 1480 – 1492.
15. Yang J.S., Liau K.L., Tu C.W., Hwang C.Y. // J. Phys. Chem. A. – 2005. – **109**. – P. 6450 – 6456.
16. Uda M., Momotake A., Arai T. // Tetrahedron Lett. – 2005. – **46**. – P. 3021 – 3024.
17. Schuster D.I., Nuber B., Vail S.A., MacMahon S., Lin C., Wilson S.R., Khong A. // Photochem. Photobiol. Sci. – 2003. – **2**. – P. 315 – 321.
18. Tatewaki H., Baden N., Momotake A., Arai T., Terazima M. // J. Phys. Chem. B. – 2004. – **108**. – P. 12783 – 12789.
19. Turro N.J. / Modern Molecular Photochemistry, The Benjamin, Cummings Publishing Co., Inc., Menlo Park (C.A) – London, Amsterdam, 1978.
20. Saltiel J., Charlton J.L. in Rearrangement in Ground, Excited states. / ed. By P. deMayo. – New York: Academic Press, 1980. – **3**. – P. 25.
21. Kirk-Othner // Encyclopedia of Chemical Technology. 4-th ed. Wiley, 1996. – **3**. – P. 25.
22. Feringa B.L. // Tetrahedron. – 1993. – **94**. – P. 8267 – 8310.
23. Braun A.M., Murette M.J., Oliveros E. // Photochemical Technology. – New York: Wiley, 1991.
24. Feringa B.L., van Delden R.A., Koumura N., Geertsema E.M. // Chem. Rev. – 2000. – **100**. – P. 1789 – 1816.
25. Balogh-Nair V., Nakanishi K. in Chemistry, Biology of synthetic Retenoids / Ed. by M. Dawson, W. Okamura. – Boca – Raton: CRC Press, 1990, FL. – P. 147.

26. Rao V.J., Derguini F., Nakanishi K., Taguchi T., Hosada A., Hanzawa Y., Kobayashi T., Pande C.M., Callender R.R. // *J. Amer. Chem. Soc.* – 1986. – **108**. – P. 6077 – 6078.
27. Liu R.S.H., Shichida Y. // *Photochemistry in Organized, Constrained Media. Chapter 18.* / Ed. V. Ramamurthy. – New York: VCH Publishers, 1991.
28. Irie M. // *Chem. Rev.* – 2000. – **100**. – P. 1685 – 1716.
29. Arai T., Karatsu T., Sakuragi H., Tokumaru K. // *Tetrahedron Lett.* – 1983. – **24**. – P. 2873 – 2876.
30. Hamaguchi H., Karatsu M.T., Arai T., Tokumaru K. // *J. Amer. Chem. Soc.* – 1986. – **108**. – P. 1698 – 1699.
31. Arai T., Tokumaru K. // *Chem. Rev.* – 1993. – **93**. – P. 23 – 39.
32. Becker H.D. // *Chem. Rev.* – 1993. – **93**. – P. 145 – 172.
33. Saltiel J., Tarkalanov N., Sears D.F. Jr. // *J. Amer. Chem. Soc.* – 1995. – **117**. – P. 5586 – 5587.
34. Saltiel J., Zhang Y., Sears D.F. Jr. // *J. Amer. Chem. Soc.* – 1996. – **118**. – P. 2811 – 2817.
35. Saltiel J., Zhang Y., Sears D.F. Jr. // *J. Amer. Chem. Soc.* – 1997. – **119**. – P. 11202 – 11210.
36. Saltiel J., Krishnamoorthy G., Sears D.F. Jr. // *Photochem. Photobiol. Sci.* – 2003. – **2**. – P. 1162 – 1168.
37. Lewis F.D., Liu X. // *J. Amer. Chem. Soc.* – 1999. – **121**. – P. 11928 – 11929.
38. Mazzucato U., Momicchioli F. // *Chem. Rev.* – 1991. – **91**. – P. 1679 – 1719.
39. Fischer G., Fischer E. // *J. Phys. Chem.* – 1981. – **85**. – P. 2611 – 2613.
40. Spalletti A., Bartocci G., Masetti F., Mazzucato U., Cruciani G. // *Chem. Phys.* – 1992. – **160**. – P. 131 – 144.
41. Bartocci G., Mazzucato U., Spalletti A. // *Chem. Phys.* – 1996. – **202**. – P. 367 – 376.
42. Ghiggino K.P., Skilton P.F., Fischer E. // *J. Amer. Chem. Soc.* – 1986. – **108**. – P. 1146 – 1149.
43. Wismontski-Knittel T., Das P.K., Fischer E. // *J. Phys. Chem.* – 1984. – **88**. – P. 1163 – 1168.
44. Arai T., Karatsu T., Sakuragi H., Tokumaru K., Tamai N., Yamazaki I. // *Chem. Phys. Lett.* – 1989. – **158**. – P. 429 – 434.
45. Kang T.J., Etheridge T., Jarzeba W., Barbara P.F. // *J. Phys. Chem.* – 1989. – **93**. – P. 1876 – 1881.
46. Brearley A.M., Strandjord A.J.G., Flom S.R., Barbara P.F. // *Chem. Phys. Lett.* – 1985. – **113**. – P. 43 – 48.
47. Karatsu T., Yoshikawa N., Kitamura A., Tokumaru K. // *Chem. Lett.* – 1994. – P. 381 – 384.
48. Krongauz V., Castel N., Fischer E. // *J. Photochem.* – 1987. – **39**. – P. 285 – 300.
49. Karatsu T., Itoh H., Nishigaki A., Fukui K., Kitamura A., Matsuo S., Misawa H. // *J. Phys. Chem. A.* – 2000. – **104**. – P. 6993 – 7003.
50. Jacobs H.J., Havinga E. // *Adv. Photochem.* – 1979. – **11**. – P. 305.
51. Birks J.B., Bartocci G., Aloisi G.G., Dellonte S., Barigelletti F. // *Chem. Phys.* – 1980. – **51**. – P. 113 – 120.
52. Bartocci G., Ginocchietti G., Mazzucato U., Spalletti A. // *Chem. Phys.* – 2006. – **328**. – P. 275 – 283.
53. Marcotte N., Fery-Forgues S. // *J. Photochem. Photobiol. A: Chemistry.* – 2000. – **130**. – P. 133 – 138.
54. Bartocci G., Spalletti A. // *J. Phys. Chem. A.* – 2002. – **106**. – P. 7068.
55. Ciorba S., Fontana F., Ciancaleoni G., Caronna T., Mazzucato U., Spalletti A. // *J. Fluorescence.* – 2009. – **19**. – P. 759.
56. Bartocci G., Galiazzo G., Ginocchietti G., Mazzucato U., Spalletti A. // *Photochem. Photobiol. Sci.* – 2004. – **3**. – P. 870.
57. Ginocchietti G., Galiazzo G., Mazzucato U., Spalletti A. // *Photochem. Photobiol. Sci.* – 2005. – **4**. – P. 547.
58. Barldi I., Benassi E., Spalletti A. // *Spectrochim. Acta Part A: Molecular, Biomolecular Spectroscopy.* – 2008. – **71**. – P. 543.
59. Bushan K.M., Rao G.V., Soujanya T., Rao V.J., Saha S., Samanta A. // *J. Org. Chem.* – 2001. – **66**. – P. 681 – 688.
60. Reddy M.J.R., Rao G.V., Manibhushan K., Reddy M.J.R., Gopal V.R., Rao V.J. // *Chem. Lett.* – 2001. – **3**. – P. 186 – 187.
61. Reddy M.J.R., Srinivas U., Srinivas K., Reddy V.V., Rao V.J. // *Bull. Chem. Soc. Jpn.* – 2002. – **75**. – P. 2487 – 2495.
62. Gopal V.R., Reddy A.M., Rao V.J. // *J. Org. Chem.* – 1995. – **60**. – P. 7966 – 7973.
63. Barbara P.F., Jarzeba W. // *Adv. Photochem.* – 1990. – **15**. – P. 1.
64. Lippert E.Z., Rettig W., Banacic-Koutecky V., Heisel F., Meihe J. // *Adv. Chem. Phys.* – 1987. – **68**. – P. 1.
65. Scaiano J.C. *Handbook of Organic Photochemistry*; CRC press: Boca Raton, FL, 1, 1989.
66. Calvert J.G., Pitts J.N. Jr. // *Photochemistry* / Eds, Wiley: New York, Chapter VII, 1966.
67. Tanaka K., Miura T., Umezawa N., Urano Y., Kikuchi K., Higuchi T., Nagano T. // *J. Amer. Chem. Soc.* – 2001. – **123**. – P. 2530 – 2536.
68. Fairbourne A. // *J. Chem. Soc.* – 1921. – **119**. – P. 1573 – 1582.
69. Traxler J.T. // *Syn. Comm.* – 1977. – **7**. – P. 161 – 166.
70. Gore P.H. // *J. Chem. Soc.* – 1959. – P. 1616 – 1618.
71. Marshall J.A., Anderson N.H., Schlicher J.W. // *J. Org. Chem.* – 1970. – **35**. – P. 858 – 861.

72. Wadsworth W.S. // *Org. React.* – 1977. – **25**. – P. 73 – 145.
73. Maryanoff B.E., Reitz A.B. // *Chem. Rev.* – 1989. – **89**. – P. 863 – 927.
74. Reddy A.M., Gopal V.R., Rao V.J. // *Ind. J. Chem.* – 1996. – **35B**. – P. 312 – 317.
75. Frisch M.J., Trucks G.W., Schlegel H.B., Scuseria G.E., Robb M.A., Cheeseman J.R., Montgomery J.A. Jr., Vreven T., Kudin K.N., Burant J.C., Millam J.M., Iyengar S.S., Tomasi J., Barone V., Mennucci B., Cosi M., Scalmani G., Rega N., Petersson G.A., Nakatsuji H., Hada M., Ehara M., Toyota K., Fukuda R., Hasegawa J., Ishida M., Nakajima T., Honda Y., Kitao O., Nakai H., Klene M., Li X., Knox J.E., Hratchian H.P., Cross J.B., Bakken V., Adamo C., Jaramillo J., Gomperts R., Stratmann R.E., Yazyev O., Austin A.J., Cammi R., Pomelli C., Ochterski J.W., Ayala P.Y., Morokuma K., Voth G.A., Salvador P., Dannenberg J.J., Zakrzewski V.G., Dapprich S., Daniels A.D., Strain M.C., Farkas O., Malick D.K., Rabuck A.D., Raghavachari K., Foresman J.B., Ortiz J.V., Cui Q., Baboul A.G., Clifford S., Cioslowski J., Stefanov B.B., Liu G., Liashenko A., Piskorz P., Komaromi I., Martin R.L., Fox D.J., Keith T., Al-Laham M.A., Peng C.Y., Nanayakkara A., Challacombe M., Gill P.M.W., Johnson B., Chen W., Wong M.W., Gonzalez C., Pople J.A. Gaussian 03 revision B.01, Gaussian, Inc., Wallingford CT, 2004.
76. Bartocci G., Masetti U., Mazzucato U., Spalletti A., Orlandi G., Poggi G. // *J. Chem. Soc., Faraday Trans.* – 1988. – **84**. – P. 385 – 399.
77. Momicchioli F., Baraldi I., Fischer E. // *J. Photochem. Photobiol. A.* – 1989. – **48**. – P. 95 – 107.
78. Reichhardt C. *Solvents, Solvent Effects in Organic Chemistry*, VCH, Weinheim, 1, 988.